On topographic controls of soil hydraulic parameter scaling at hillslope scales

Raghavendra B. Jana[1] and Binayak P. Mohanty[1]

Received 27 July 2011; revised 28 November 2011; accepted 5 January 2012; published 18 February 2012.

[1] Most upscaling efforts for soil hydraulic parameters developed thus far have opted to ignore the effect of topography in their derivation of effective parameter values. This approach, which considers a flat terrain with no lateral flows, is reasonable as long as the coarser support dimensions are of the order of a few hundred meters. In such a scenario, the upscaled characteristics of the parameters are governed predominantly by the texture and structure of the soil in the domain. However, when upscaling fine-scale hydraulic parameter data to much larger extents (hillslope scales and beyond), topography plays a bigger role and can no longer be ignored. Efforts to model hydrologic processes and phenomena, with particular emphasis on those occurring in the unsaturated zone, are conducted at various scales. We present here a study to isolate the influence of topographic variations on the effective, upscaled soil hydraulic parameters under different hillslope configurations. The power-averaging operator algorithm was used to aggregate fine-scale soil hydraulic parameters to coarser resolutions. Hydrologic scenarios were simulated using HYDRUS-3D for four different topographic configurations under different conditions to test the validity of the upscaled soil hydraulic parameters. The outputs from the simulations (fluxes and soil moisture states) were compared across multiple scales for validating the effectiveness of the upscaled soil hydraulic parameters. It was found that the power-averaging algorithm produced reasonably good estimates of effective soil hydraulic parameters at coarse scales. Further, a probable threshold dimension beyond which the topography dominates the soil hydraulic property variation was analyzed. On the basis of only the topography, the scaling algorithm was able to capture much of the variation in soil hydraulic parameters required to generate equivalent flows and soil moisture states in a coarsened domain.

Citation: Jana, R. B., and B. P. Mohanty (2012), On topographic controls of soil hydraulic parameter scaling at hillslope scales, *Water Resour. Res.*, *48*, W02518, doi:10.1029/2011WR011204.

1. Introduction

[2] Scaling of soil hydraulic parameters is urgently necessary for better performance of many hydrological, meteorological, and ecological models. Often the requisite data are measured at a scale inconsistent with the inherent scale at which these models work. Hence, there is a need for scaling schemes which enable one to convert available measured fine resolution data to effective coarser resolution aggregate values or vice versa. Interconnections often exist between information across these scales [*Wu and Li*, 2006]. Understanding how hydraulic parameters are affected at different scales by the spatial variability of influencing factors such as soil structure and texture, vegetation, and topography is an inherent requirement of efficient scaling schemes. While it is known that connections exist between these factors and the hydraulic parameters, the exact mathematical and/or physical nature of these connections is generally unknown. Over the past few decades, numerous efforts have been made to either understand these connections and solve the unknowns, or to find a way around them so as to obtain effective parameters at multiple scales.

[3] Upscaling is the process of replacing a domain of heterogeneous soil properties with an effective, homogeneous one. Most upscaling efforts for soil hydraulic parameters published thus far [e.g., *Khaleel et al.*, 2002; *Mohanty and Zhu*, 2007; *Vereecken et al.*, 2007, and references therein; *Yeh et al.*, 2005; *Zhu and Mohanty*, 2002a, 2002b, 2002c, 2003, 2004, 2006; *Zhu et al.*, 2004, 2006] have opted to ignore the effect of topography in their derivation of effective parameter values. This approach, which considers a flat terrain, with no lateral flows, is reasonable when the coarser support dimensions are of the order of a few hundred meters (field scale). Here, the term "support" refers to the area (or volume) for which the parameter value is valid [*Bloschl and Sivapalan*, 1995]. In such a scenario, the upscaled characteristics of the parameters are governed predominantly by the texture and structure of the soil in the domain. However, when upscaling fine-scale hydraulic parameter data to much larger extents (hillslope scales and beyond), topography plays a bigger role and can no longer be ignored. Lateral flows occur within the vadose zone because of topographic variations. Additionally, surface runoff and run on also occur. Going deeper into the causes of variation of soil hydraulic properties in space, it can be

[1]Department of Biological and Agricultural Engineering, Texas A&M University, College Station, Texas, USA.

0043-1397/12/2011WR011204

argued that the topography plays a vital role in determining the soil formation and deposition patterns [*Kohnke and Franzmeier*, 1995]. It has been known since the 1950s that topography plays a critical role in classification of soils. *Lag* [1951] and *Tedrow* [1951] conducted field studies to show that soils having similar morphological and genetic histories and that are subjected to similar crop practices displayed different drainage properties on the basis of the topography and the position of the soil within the landscape. Soil layer depths vary from location to location. Generally, valleys have deeper soil profiles above the bedrock than locations at higher elevations where the soil depth is determined by the slope steepness [*Hillel*, 1991]. In a study of five catchment areas in Australia and New Zealand [*Wilson et al.*, 2004], it was found that the topography and the spatial variation of soil properties and vegetation played equally important roles in the variability of soil moisture patterns. *Western et al.* [2004] also found that the topography played a dominant role in dictating soil moisture patterns as compared to soil hydraulic parameter variability at some sites in the same study areas. *Seibert et al.* [2007] analyzed soils data from the Swedish National Forest Soil Inventory to validate that, at the landscape scale, topography is important in dictating soil formation and deposition, and hence, their properties. Correlations between topographic indices and soil physical and chemical properties were analyzed in the study. *Pradhan et al.* [2006] showed that the value of the topographic index used in TOPMODEL [*Beven et al.*, 1984] was dependent on the resolution of the DEM from which it was derived. A marked shift toward higher topographic index values was observed in conjunction with increase in the coarseness of the DEM resolution from 50 m to 1000 m. This phenomenon was attributed to the loss of high-frequency topographic information (or microtopography) in the coarser DEMs. *Zhang and Montgomery* [1994] also studied the effect of DEM grid size on land surface and hydrologic simulations, and reached the conclusion that the 10 m grid size was a "reasonable compromise" between the need for fine-grained accuracy and the demands of a high data volume. In another study on the application of the MIKE-SHE model using different grid sizes, *Vazquez et al.* [2002] found that the finest resolution used did not necessarily result in the best validation results for river discharge. On the basis of the multiple resolutions used between 300 and 1200 m, they concluded, keeping in mind the computation time and the validation of river discharge, that the 600 m grid resolution was the most appropriate for their study catchment. *Kuo et al.* [1999] found that the choice of grid size had a greater effect during the dry periods of simulation, as compared to the wet periods. They also found that using large grid sizes resulted in misrepresentation of the curvature of the topography.

[4] Thus, adopting the flat-terrain assumption to scaling of soil hydraulic parameters may be reasonable at smaller scales and in cases with hypothetical situations used to derive analytical solutions for the scaling problem. However, real-world applications of scaling schemes demand that the physical controls influencing soil parameter values be incorporated into these schemes. Such scenarios warrant the inclusion of the effect of topography in the upscaling algorithm when considering large extents [*Mohanty and Mousli*, 2000]. We present here a study to isolate the influence of topographic variations on the effective, upscaled soil hydraulic parameters under different hillslope configurations. The objective of the study was to examine the scale dependency of soil hydraulic parameters such as the saturated hydraulic conductivity, the saturation and residual soil water contents, and the van Genuchten parameters, at the hillslope scale while incorporating the influence of the physical controls such as the topography and vegetation into the scaling algorithms.

[5] Throughout this article, we refer to scaling, upscaling, and aggregation interchangeably. Upscaling is a term which signifies the direction of the scaling being applied. Hence, the uses of the two terms do not indicate different processes. The term "aggregation" has been used differently by some researchers. *Kabat et al.* [1997] defined aggregation as an areal weighted averaging of the soil texture for the domain, and then assigning hydraulic parameter values to this new texture. *Niedda* [2004] considered the averaging of the digital elevation model with coarsening of the scale as aggregation. In these cases, the term aggregation was used as distinct from upscaling. However, in our study, we do not aggregate either the soil texture or the elevation data for the domain. Rather, the soil hydraulic parameters themselves are aggregated at the coarse scales to provide effective values. As explained by *Vereecken et al.* [2007], upscaling is the process of replacing a domain of heterogeneous soil parameter values with a single effective homogeneous value. As such, any algorithm that achieves this objective, including aggregation of soil hydraulic parameters, can be termed an upscaling algorithm [*Hopmans et al.*, 2002; *Shouse and Mohanty*, 1998].

2. Mathematical Framework and Domain Setup

2.1. Power Average Operator

[6] The power average operator, as described by *Yager* [2001], was used in this study to coarsen the soil hydraulic parameter values. Two types of aggregation methods are combined in this technique. In mode-like methods, the emphasis is on finding the most probable value of a parameter from a given set [*Yager*, 1996]. In mean type aggregation, the goal is to find the average value of the given set. By combining the features of both the aggregating methods, the power average technique provides itself as an ideal tool for use in scaling of soil hydraulic parameters. Generally, soil pedons clustered around a location tend to have similar properties, with the spatial correlation dying out as the distance between two points increases. This means that the aggregating method must take into consideration the mutual support the pedons extend to each other when clustered. The power average operator allows for such an aggregation of clustered data to combine in a nonlinear fashion to support each other.

[7] The power average operator is defined as

$$P^*(p_1, p_2, \ldots, p_{1,}) = \frac{\sum_{i=1}^{n} \Big(1 + T(p_i)\Big) p_i}{\sum_{i=1}^{n} \Big(1 + T(p_i)\Big)}. \tag{1}$$

where

$$T(p_i) = \sum_{\substack{j=1 \\ j \neq i}}^{n} \mathrm{Sup}(p_i, p_j). \tag{2}$$

P^* is the power average of the parameter values $p_i, \ldots, p_n$, where n is the total number of nodes being aggregated. Sup(p_i, p_j) is the support for p_i from p_j. This feature allows data clustered around a particular value to combine nonlinearly while being aggregated. The support function is the crux of the power average method. Generally, the support function is required to adhere to the following three properties [*Yager*, 2001]:

$$\mathrm{Sup}(p_i, p_j) \in [0, 1];$$

$$\mathrm{Sup}(p_i, p_j) = \mathrm{Sup}(p_j, p_i);\ \frac{-b \pm \sqrt{b^2 - 4ac}}{2a};$$

$$\mathrm{Sup}(p_i, p_j) \geq \mathrm{Sup}(p_x, p_y) \text{ if } |p_i - p_j| < |p_x - p_y|.$$

The third condition means that the closer the values are, the more they support each other. When p_i is very close to p_j (i.e., $p_i \approx p_j$), Sup(p_i, p_j) $\rightarrow$ 1 and $P^* = p_i$. When p_i is very far from p_j, Sup(p_i, p_j) $\rightarrow$ 0, and P^* turns out to be the arithmetic average.

[8] A general form of the support equation is given by

$$\mathrm{Sup}(p_i, p_j) = e^{-\eta(p_i - p_j)^2} \tag{3}$$

where $\eta \geq 0$. This function is continuous, symmetric and lies in the unit interval, as required. It can be seen that as $p_i = p_j$, the support value equals 1, and as the difference becomes large, the support tends to 0. The power law form of the support function is similar to the form of the transmissivity profile used in the generalized form of the TOPMODEL algorithm to compute the topographic index [*Iorgulescu and Musy*, 1997].

[9] In our application of the power-averaging operator to scaling of soil hydraulic parameters, η may be thought of as a scale parameter. As such, in nature η can be influenced by many factors such as the difference in elevation, distance between observations, variations in atmospheric forcings, changes in vegetation, soil texture and structure. In this study, we constrained the other factors so that η could be defined as a function of only the elevation differential and the distance between observations. The value of η was given by the formula

$$\eta = \left(\frac{z_{j_{\max}} - z_{j_{\min}}}{z_i - z_j}\right)^2 * \frac{\sqrt{(x_i - x_j)^2 + (y_i - y_j)^2 + (z_i - z_j)^2}}{S} \tag{4}$$

Here x, y, and z are the Cartesian coordinates of the point, while S is the scale (resolution) to which the hydraulic parameters are being aggregated. The first term on the right-hand side is the normalized difference in elevation between the two locations i and j. The second term provides the linear distance between measurement values, normalized by the scale dimension. A distance which may be considered as "far" at one scale may not be so at a coarser scale. Hence, normalizing the actual distance by the scale dimension provides a more meaningful way of computing the support function. The linear distance between points by itself does not really give an indication of the topographic variability. Two points far apart in the X-Y direction and having no difference in the Z direction could have the same linear distance between them as points closer to each other in the X-Y direction but with a large difference in their Z coordinates. Hence, the elevation difference was considered separately to isolate the elevation differential which gives an indication of the topographic variability of the domain. Further, this term was squared to give a greater weight to it as compared to the linear distance alone. Implications of using the linear distance in all study cases are given in section 3.

2.2. Physical Domain Setup

[10] The physically based HYDRUS-3D hydrologic simulation software [*Šimůnek et al.*, 2006] was used to validate the upscaling scheme. The HYDRUS-3D software package solves the Richards' equation for water flow in saturated/unsaturated domains using numerical techniques. The governing flow equation is a modified form of the Richard's equation given as

$$\frac{\partial \theta}{\partial t} = \frac{\partial}{\partial x_i}\left[K\left(K_{ij}^A \frac{\partial h}{\partial x_j} + K_{iz}^A\right)\right] - S \tag{5}$$

where θ is the volumetric water content, h is the pressure head, S is a sink term, x_i (i = 1, 2) are the spatial coordinates, t is time, K_{ij}^A are components of a dimensionless anisotropy tensor K^A, and K is the unsaturated hydraulic conductivity, given by

$$K(h, x, y, z) = K_s(x, y, z) K_r(h, x, y, z) \tag{6}$$

where K_r and K_s are the relative and saturated hydraulic conductivities, respectively.

[11] The HYDRUS-3D software allows the user to analyze water flow through saturated, partially saturated or unsaturated regions with irregular boundaries, and composed of nonuniform soils. HYDRUS-3D allows for three dimensional flow representations in the unsaturated zone. However, the 3-D version of HYDRUS does not allow for inverse estimation of soil hydraulic parameters from flux data. This feature is available only in the l-D and 2-D versions of this software. *Kampf and Burges* [2007] used the HYDRUS-2D model to inversely estimate the soil hydraulic parameters for a hillslope study area in the Panola Mountain Research Watershed of Georgia where the hydrologic responses were measured. Since we intended to consider a more realistic view of the water flow process involved in a hillslope, we decided to use the HYDRUS-3D model, even though it had the drawback of not providing an easy means of inverse parameter estimation. Hence, our approach of upscaling the soil hydraulic parameters is using a topography-based aggregation scheme, and then comparing the domain responses using these upscaled parameters with those obtained using the fine-scale soil hydraulic parameters. The upscaling algorithm was tested under multiple scenarios to validate its applicability under different conditions with respect to topography, soil distribution, land cover, and water table elevations.

2.3. Topographic Configurations

[12] Four plots of 1000 m $\times$ 1000 m (Figure 1) were generated to represent hillslopes with four specific topographic

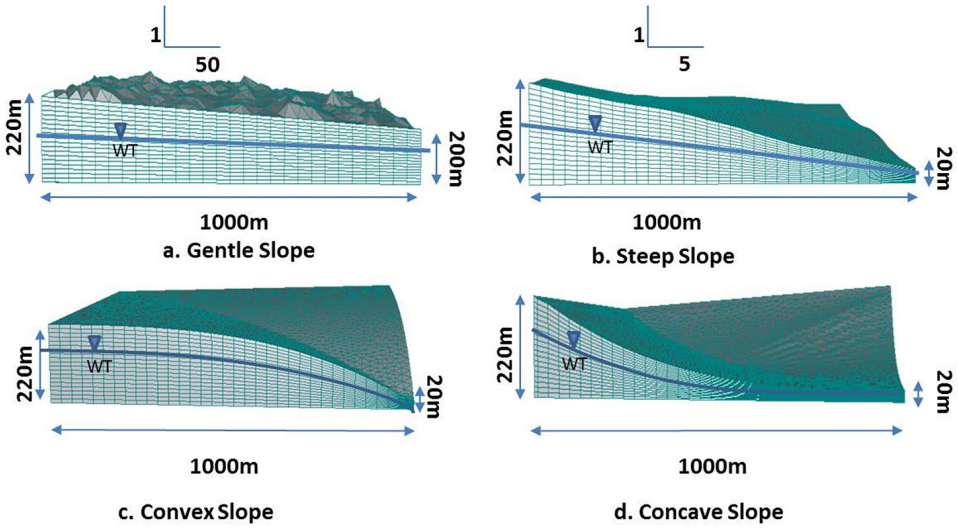

Figure 1. Topographic configurations. (a) Gentle uniform slope, (b) steep uniform slope, (c) convex slope, and (d) concave slope.

configurations. Figure 1a had a uniform slope of 1:50 (gentle slope). The second plot had a steeper uniform slope of 1:5. The third plot had a slope with a convex curvature while the fourth plot featured a concave slope geometry. In all configurations, a maximum relief of 200 m and minimum domain thickness of 20 m were maintained. Microtopography was generated for the surfaces using the HydroGen random field generator software [*Bellin and Rubin*, 1996].

2.4. Soils

[13] Loam, loamy sand, sand, sandy clay loam, sandy loam, silty clay loam, and silt loam were used in this study. Soil hydraulic parameter values attributed to these soils, the residual water content (θ_r), saturation water content (θ_s), van Genuchten parameters (α and n), and the saturated hydraulic conductivity (K_s), were obtained from the ROSETTA [*Schaap et al.*, 2001] framework embedded in HYDRUS-3D. A parallel stream tube approach was considered and the soils did not vary with depth. The choice of uniform soils with depth is justified by the fact that the spatial extent of the study domain in the horizontal directions (1 km × 1 km) was much greater than the vertical profile (maximum of 220 m and minimum of 20 m). Hence, changes in the soil properties due to layering can be assumed to be minor.

2.5. Land Cover Configurations

[14] The performance of the upscaling algorithm was tested with four different land cover types in this study. The four scenarios had bare soil, grass, corn, and deciduous fruit trees as vegetation cover. Corresponding suitable evapotranspiration values were assigned within HYDRUS-3D to simulate these land cover types. The bare soil had no transpiration, and only evaporation values were used. Adjustments (crop factors) were incorporated into the transpiration values for the corn and deciduous fruit trees' growing seasons, while the grass cover had a transpiration rate along with the evaporation of the bare soil for most of the year, dying off in the winter months. Figure 2 shows the evapotranspiration (ET) patterns for the four land cover cases. These potential ET values were obtained from the Texas High Plains Evapotranspiration Network so as to provide realistic data for the numerical simulations and then multiplied with a crop factor for the corresponding land cover. The bimodal ET pattern for the fruit trees indicates a mix of tree types with different growing seasons.

2.6. Water Table

[15] Four water table levels were assigned to each of the topographic scenarios. Configurations with water tables at 2–4 m, 8–10 m, and 18–20 m were simulated, along with a scenario where no water table (i.e., free drainage) was assigned. These water table depths were selected to depict shallow, deep, and very deep groundwater levels. Within the ranges mentioned above, the water tables varied with the depth, i.e., locations with lower surface elevation had shallow water tables, while locations at higher elevations had deeper water tables.

2.7. Finite Element Mesh and Initial Material Distribution

[16] Finite element meshes were generated for each hillslope plot with 20 horizontal layers and lateral node spacing of 30 m. The number of nodes and elements in the finite element mesh (FEM) varied slightly according to the topographic configuration. The top surface was assigned a time-dependent "atmospheric boundary" condition, while the cross-sectional boundaries along the periphery of the soil plot were designated as seepage faces. The atmospheric boundary condition is system dependent and can switch between flux and head type conditions, depending on external conditions and the existing soil moisture conditions of the domain. Equation (5) can be numerically solved while restraining the absolute flux value such that two conditions are met:

$$\left| K\left(K_{ij}^{A}\frac{\partial h}{\partial x_j}+K_{iz}^{A}\right)n_i\right| \le E \tag{7}$$

$$h_{\min} \le h \le h_{\max} \tag{8}$$

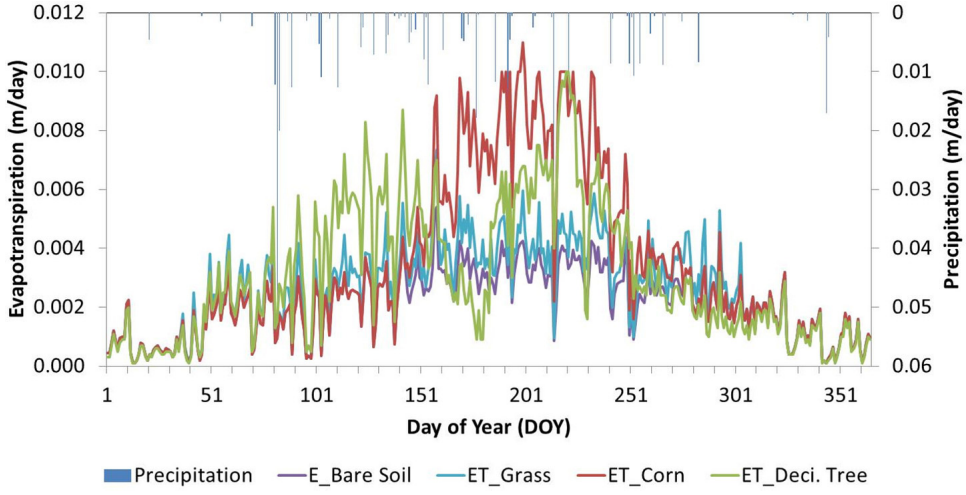

Figure 2. Evaporation and evapotranspiration patterns for the four land cover cases, along with the precipitation pattern.

where E is the maximum potential rate of infiltration or evaporation, h is the soil surface pressure head, and h_{max} and h_{min} are the maximum and minimum pressure heads allowed for the particular soil conditions of the domain, and n_i are the components of the outward unit vector normal to the boundary. h_{min} is determined by the equilibrium between the soil moisture and atmospheric water vapor, while h_{max} is usually set to zero.

[17] A seepage face boundary condition is similar to the atmospheric boundary condition, except that the pressure head is held constant at $h = 0$. This enables flow of water out of the node only if the corresponding region of the soil domain is saturated (i.e., $h \geq 0$). This is also a time-dependent boundary condition. The bottom boundary had a free drainage condition (gravity drainage) for the case with no assigned water table, while the other water table cases had a variable head boundary condition at the bottom.

[18] Initial conditions of the soil profile above the water table were given as a soil water content of 0.30 v/v. Time-dependent boundary conditions such as precipitation, evaporation, and transpiration values were assigned for the domain for a period of 365 days, the duration for which the water flow was simulated in the soil domains. These conditions were held constant across all topographic scenarios to ensure similar conditions.

[19] Initially, each node in the FEM was randomly assigned one of the soil types mentioned in section 3.4. Table 1 contains details of soil hydraulic parameter values assigned initially to the FEM nodes. Root water uptake parameters were also assigned for the Feddes model, with no solute stress and a maximum rooting depth of 1 m.

Table 1. Initial Soil Hydraulic Parameter Values at 30 m Resolution From ROSETTA

Soil Type	θ_r (v/v)	θ_s (v/v)	α (m^{-1})	n	K_s (m d^{-1})
Loam	0.078	0.430	3.600	1.560	0.250
Loamy sand	0.057	0.410	12.400	2.280	3.502
Sand	0.045	0.430	14.500	2.680	7.128
Sandy clay loam	0.100	0.390	5.900	1.480	0.314
Sandy loam	0.065	0.410	7.500	1.890	1.061
Silty clay loam	0.089	0.430	1.000	1.230	0.017
Silt loam	0.067	0.450	2.000	1.410	0.108

[20] The power-averaging algorithm, described in section 2.1, was applied to aggregate five soil hydraulic parameters: residual soil water content (θ_r), saturation water content (θ_s), van Genuchten parameters α and N, and the saturated hydraulic conductivity, K_s. These parameters were aggregated from 30 m to resolutions of 60, 90, 120, and 240 m. This is similar to 2X, 3X, 4X, and 8X the original resolution. Rather than coarsening the FEM grid to reflect the coarser resolution distributions, we assigned the aggregated effective soil hydraulic parameters to each node within the upscaled pixel footprint. This was done so that the computational integrity of the FEM would be consistent across all scales. It must be noted that while the soil types or hydraulic parameter values are assigned by the user to the nodes, the HYDRUS program interpolates the values to the 3-D elements in the mesh. On the basis of the number of nodes in the FEM domain (which in turn is based on the topographic configuration), the number of materials obtained at each scale were slightly different for each topographic scenario. However, for each plot type, there was a reduction in the number of materials with each successive upscaling. This is logical since we were homogenizing the variety of soils into one effective soil type for the entire coarse-scale pixel. Hence, the larger the pixel size is, the smaller the number of pixels (and thus effective soil types) necessary to cover the entire domain is.

3. Results and Discussion

[21] Five soil hydraulic parameters, θ_r, θ_s, α, n, and K_s, were upscaled using the power-averaging operator from 30 m resolution to 60, 90, 120, and 240 m resolutions. The "effective" parameters at each resolution were used to simulate the soil domain using the physically based hydrologic modeling software, HYDRUS-3D. Results from these simulations were analyzed across different scales, times, and configurations to assess the "effectiveness" of the upscaled

Table 2. Descriptive Statistics of Upscaled Soil Hydraulic Parameters

		Scale									
		30 m (N = 1086)		60 m (N = 289)		90 m (N = 121)		120 m (N = 81)		240 m (N = 25)	
	Parameter	Mean	SD	Mean	SD	Mean	SD	Mean	SD	Mean	SD
Flat terrain	θ_r	0.071	0.017	0.070	0.017	0.069	0.017	0.068	0.017	0.068	0.018
	θ_s	0.421	0.018	0.421	0.017	0.423	0.016	0.422	0.016	0.424	0.014
	van Genuchten α	6.935	4.837	7.238	4.919	7.429	5.199	7.646	5.200	7.581	5.682
	van Genuchten n	1.813	0.492	1.841	0.496	1.866	0.518	1.887	0.521	1.899	0.581
	K_s	1.875	2.493	1.994	2.490	2.176	2.568	2.268	2.603	2.518	2.936
Gentle slope	θ_r	0.076	0.003	0.075	0.002	0.075	0.001	0.075	0.001	0.075	0.001
	θ_s	0.423	0.004	0.423	0.002	0.423	0.001	0.423	0.002	0.424	0.001
	van Genuchten α	3.247	0.842	3.175	0.482	3.154	0.312	3.149	0.306	3.235	0.324
	van Genuchten n	1.504	0.073	1.507	0.041	1.508	0.026	1.511	0.025	1.519	0.022
	K_s	0.315	0.141	0.312	0.079	0.314	0.051	0.319	0.050	0.340	0.049
Steep slope	θ_r	0.075	0.002	0.075	0.001	0.075	0.001	0.076	0.001	0.076	0.000
	θ_s	0.423	0.003	0.423	0.001	0.423	0.001	0.423	0.001	0.423	0.000
	van Genuchten α	3.274	0.577	3.226	0.286	3.261	0.269	3.305	0.279	3.687	0.251
	van Genuchten n	1.500	0.052	1.505	0.024	1.511	0.019	1.515	0.017	1.535	0.009
	K_s	0.310	0.097	0.311	0.048	0.324	0.045	0.335	0.044	0.398	0.031
Convex slope	θ_r	0.076	0.004	0.076	0.004	0.076	0.003	0.076	0.002	0.076	0.001
	θ_s	0.423	0.005	0.423	0.005	0.423	0.005	0.422	0.003	0.422	0.002
	van Genuchten α	3.361	1.018	3.333	0.941	3.331	0.871	3.318	0.663	3.449	0.434
	van Genuchten n	1.506	0.092	1.510	0.081	1.516	0.071	1.516	0.051	1.528	0.029
	K_s	0.329	0.174	0.333	0.158	0.339	0.143	0.341	0.106	0.369	0.065
Concave slope	θ_r	0.076	0.003	0.076	0.002	0.076	0.001	0.076	0.001	0.076	0.000
	θ_s	0.423	0.005	0.423	0.002	0.423	0.002	0.423	0.001	0.423	0.001
	van Genuchten α	3.274	0.889	3.191	0.433	3.180	0.328	3.195	0.291	3.330	0.307
	van Genuchten n	1.506	0.077	1.508	0.037	1.510	0.027	1.512	0.022	1.521	0.014
	K_s	0.324	0.149	0.318	0.072	0.322	0.054	0.327	0.046	0.353	0.041

parameter values. We discuss in detail here the results of the cases with the grass cover, with no assigned water table.

[22] The upscaled soil hydraulic parameters for a domain with no topographic relief, i.e., a flat terrain, as obtained by using the power-averaging operator are given in Table 2. In this case, the scale parameter, η, becomes zero, and the support becomes 1. This case is provided as a base case to compare the rest of the topographic scenarios with. Table 2 also provides the descriptive statistics of the five soil hydraulic parameters at each pixel resolution for the four topographic scenarios. While the mean values for each parameter remained roughly similar at each scale for each topographic configuration, the standard deviations successively reduced with increasing coarseness. This indicates that with increasing coarseness of the scale dimension, there is reduced variability in the soil properties, and the values tend toward a single effective value. It may be observed that the K_s values generally increased with increase in coarseness of the scale. This could be explained by considering the structure of the power-averaging algorithm. In conventional arithmetic averaging (simple mean), all values are weighed equally. However, the nature of the power-averaging operator is such that the values closer to the node under consideration have greater influence on the aggregate, while those further away from the node are weighed less. This means that if a node with higher K_s value is close to the node under consideration, it would be weighed greater, thus nudging the aggregate toward a higher value. In nature, as scale increases, the occurrence of macropores and fractures also increases, thus nudging the conductivity toward higher values. Further, it is seen that, with the inclusion of the topographic relief into the scaling algorithm, the effective values of the soil hydraulic parameters were significantly different from those of the flat terrain case. The values presented for the flat terrain were driven purely by the heterogeneity in the soil properties, while those for the other topographic scenarios were driven by both soil and topographic heterogeneities. This difference in the values shows that the effective soil hydraulic parameters are indeed influenced by the topography.

3.1. Comparison of Ensemble Fluxes Across Scales for the Same Topographic Scenario

[23] Figure 3 shows an example plot of the simulated flux at the atmospheric boundary (top surface). In Figure 3, positive values connote fluxes out of the soil domain (upward), and negative values mean fluxes into the domain (downward). A similar plot is also provided for the root water uptake flux (Figure 3). The bottom boundary flux is shown in Figure 4, and the seepage flux is plotted in Figure 5. Figures 4 and 5 show the average flux values across the entire domain at the particular boundaries, with respect to time, for the scenario with grass cover and no assigned water table. It was seen that there were slight variations in these response signatures on the basis of the topography.

[24] The atmospheric flux signature shown in Figure 3 is similar to those for all four topographic scenarios. This is because the atmospheric forcings such as precipitation, evaporation and transpiration are the same across all the cases. Similarly, the root water uptake flux signatures are similar to that shown in Figure 3 because the rooting depth and the transpiration rates were similar in all cases. In Figures 4 and 5, the effect of the topographic configuration is seen. The depth of soil through which water has to pass

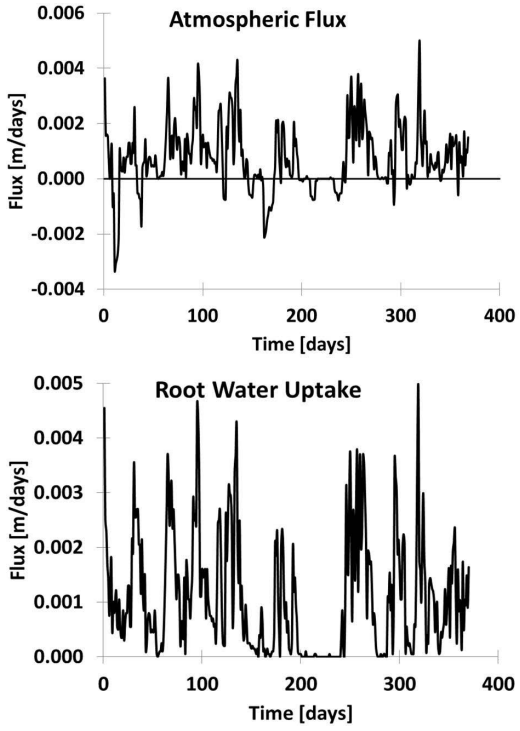

Figure 3. Example plots for atmospheric flux and root water uptake.

is different in each scenario. Hence, the amount of storage within the domain is also different. This causes the drainage flux to vary both in quantity and time. This reasoning is true for the seepage face fluxes too. The stabilization of the bottom (Figure 4) and seepage face (Figure 5) fluxes in some of the domains toward the latter part of the simulation period is caused by the low infiltration into the domain. As can be seen from the atmospheric fluxes (Figure 3), very little water entered the domain during this time because of lower rainfall. Hence, with time, the amount of water reaching the bottom and seepage faces of the domain stabilized to a constant value controlled by the unsaturated hydraulic conductivities.

[25] The surface runoff generated by the domains is not computed in the current version of HYDRUS-3D. However, it is possible to compute the volumes off-line as the difference between the infiltration capacity and the precipitation. A plot of the cumulative surface runoff thus computed for the four topographic scenarios is shown in Figure 6, which is representative of the runoff signatures at all the scales studied. The effect of the topographic configuration is apparent in this plot too. The scenario with a concave slope had the least soil depth in the domain. As a result, saturation of the domain was achieved much faster, resulting in higher surface runoff volumes. The domain with steep uniform slope generated the second highest surface runoff, while those with the gentle uniform slope and the convex slope generated the least. The gentle and convex slope domains had significantly higher soil volumes, and hence, their water retention capacity (volume) was also higher.

[26] Similar plots were obtained for the simulations scenarios with equivalent soil hydraulic parameters obtained at 60, 90, 120, and 240 m scales. For the aggregated soil hydraulic parameters at the coarse scale to be considered equivalent to the fine scale parameters, they should produce similar ensemble fluxes when compared to those with the fine-scale parameters. In order to verify this, statistical

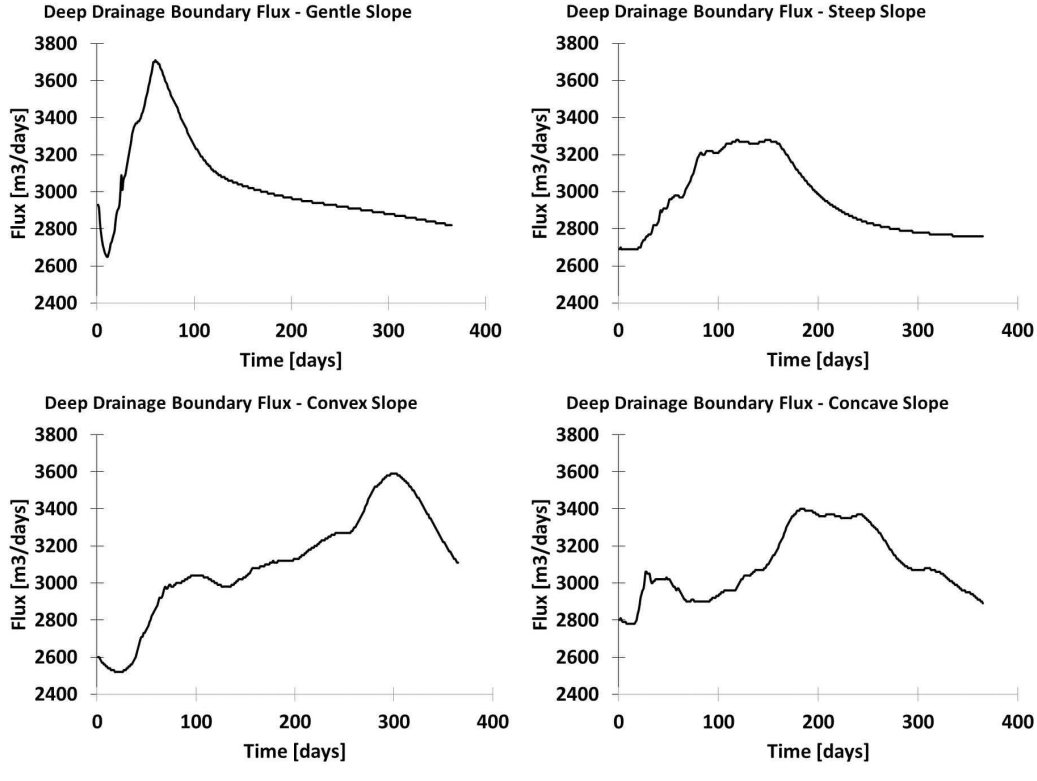

Figure 4. Drainage boundary fluxes for the four different topographic configurations.

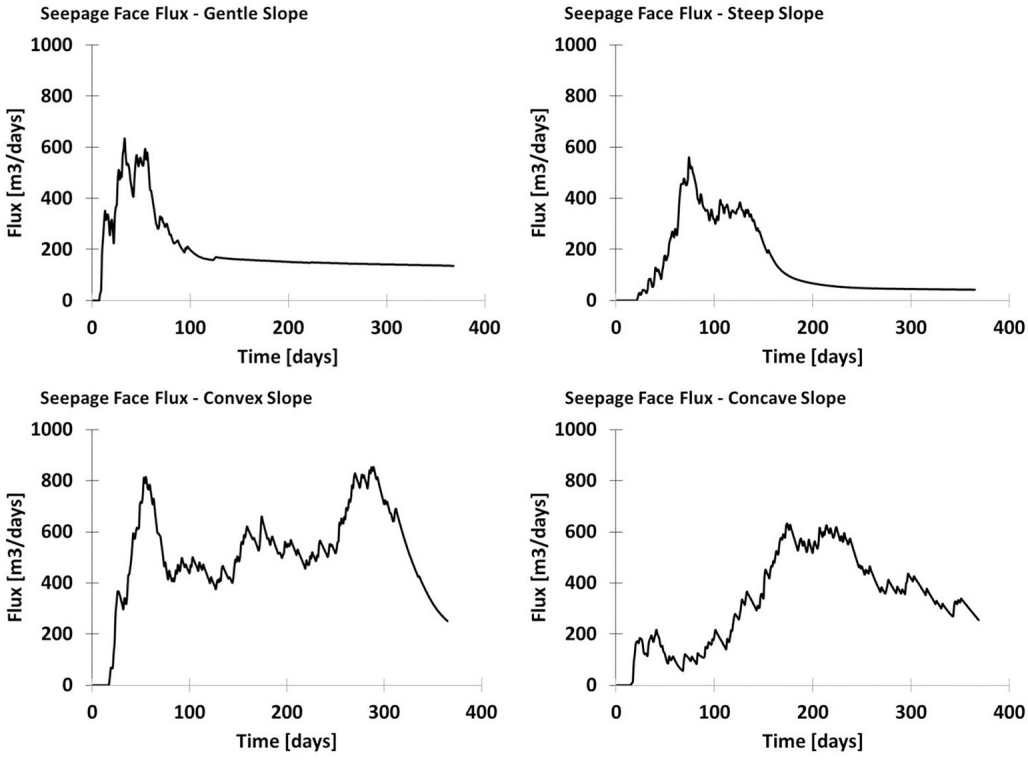

Figure 5. Seepage face fluxes for the four different topographic configurations.

analyses of the atmospheric, root water uptake, drainage, and seepage flux values were made for Pearson's R, which provides a measure of correlation, and the root mean square error (RMSE) which provides a measure of the bias. For the remainder of this paper, correlation implies Pearson's correlation, R. These comparative statistics are provided in Table 3. For all the scenarios, a very high correlation of the fluxes at the coarser resolutions with those at the 30 m scale was obtained, along with low RMSE values. The atmospheric and root water uptake flux correlations were near perfect for all topographic configurations. The bottom boundary and seepage fluxes were slightly less correlated

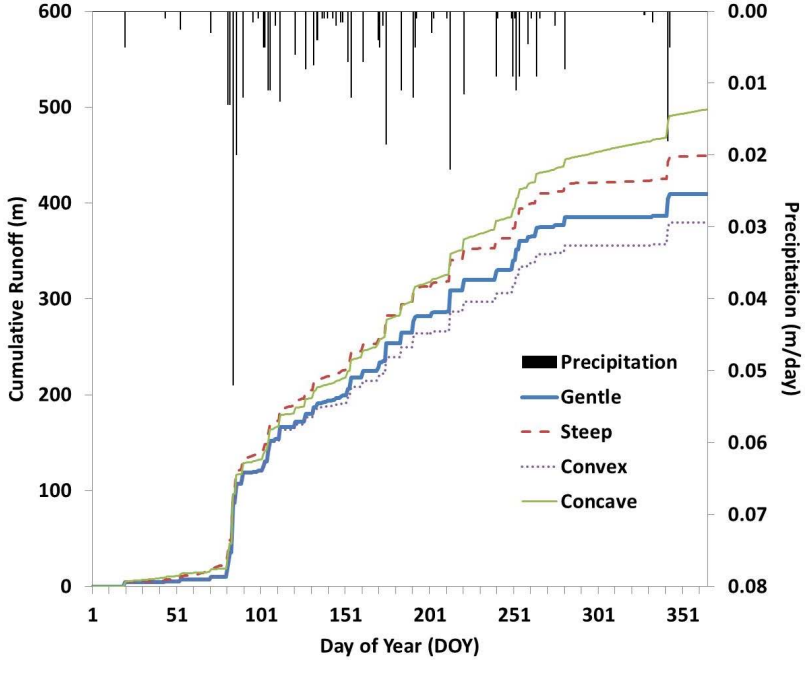

Figure 6. Cumulative runoff from the study domain for the four topographic scenarios.

Table 3. Comparative Statistics for All Fluxes Using Scaled Parameters Against Using Unscaled (30 m) Parameters[a]

		Parameter Scale							
		60 m		90 m		120 m		240 m	
	Slope	R	RMSE	R	RMSE	R	RMSE	R	RMSE
Atmospheric flux	gentle	1.000*	1.16E−4	1.000*	1.16E−4	1.000*	1.26E−4	1.000*	1.31E−4
	steep	0.991*	1.15E−4	0.991*	1.18E−4	0.991*	1.21E−4	0.991*	1.25E−4
	convex	1.000*	1.19E−4	1.000*	1.26E−4	1.000*	1.30E−4	1.000*	1.37E−4
	concave	0.991*	1.21E−4	0.991*	1.24E−4	0.991*	1.24E−4	0.991*	1.26E−4
Root water uptake	gentle	1.000*	1.29E−4	1.000*	1.29E−4	1.000*	1.39E−4	1.000*	1.39E−4
	steep	0.995*	1.27E−4	0.996*	1.32E−4	0.996*	1.33E−4	0.995*	1.37E−4
	convex	1.000*	1.31E−4	1.000*	1.33E−4	1.000*	1.35E−4	1.000*	1.41E−4
	concave	0.994*	1.38E−4	0.995*	1.38E−4	0.995*	1.38E−4	0.995*	1.42E−4
Drainage flux	gentle	0.971*	2.30E+2	0.994*	2.38E+2	0.957*	2.35E+2	0.985*	2.44E+2
	steep	0.966*	2.25E+2	0.973*	2.37E+2	0.980*	2.39E+2	0.984*	2.39E+2
	convex	0.990*	2.27E+2	0.994*	2.33E+2	0.991*	2.34E+2	0.990*	2.37E+2
	concave	0.984*	2.31E+2	0.985*	2.32E+2	0.985*	2.36E+2	0.985*	2.41E+2
Seepage face flux	gentle	0.976*	1.79E+1	0.950*	1.95E+1	0.974*	1.94E+1	0.953*	1.96E+1
	steep	0.962*	1.79E+1	0.957*	1.90E+1	0.974*	1.92E+1	0.959*	2.03E+1
	convex	0.927*	1.93E+1	0.917*	1.91E+1	0.920*	1.93E+1	0.924*	1.98E+1
	concave	0.979*	1.85E+1	0.956*	1.87E+1	0.973*	1.99E+1	0.983*	2.05E+1

[a]An asterisk (*) indicates correlations significant at the 0.01 level. R, Pearson's correlation coefficient; RMSE, root mean square error (m d^{-1}).

across the scales for all topographic configurations. As before, this is explained by the constancy of the atmospheric forcings and the rooting depth. Also, the bottom and seepage boundary fluxes were more dependent on the storage characteristics of the soil in the domain. On the other hand, the atmospheric flux was dependent on only the near-surface layers and the ambient conditions of the soil-air interface. Similarly, root water uptake was dependent on the vegetation characteristics, which were similar across the domain. All correlations had a very low p value, indicating that they were statistically significant at the 0.01 level. The low RMSE values for all boundary and vegetation fluxes show that there was no significant bias between the fluxes obtained using scaled and unscaled (30 m) soil hydraulic parameters. This, along with the high R value, indicates that the topography-based upscaling scheme has indeed resulted in equivalent soil hydraulic parameter values at the coarser scales.

3.2. Comparison of Soil Moisture States Across Time for the Four Topographic Scenarios

[27] Along with the comparison of the fluxes, comparisons of the soil moisture state of the soil domain were made at different times during the simulation period. As expected, the variability in soil moisture on a wet day, i.e., after four days of intense rainfall, was insignificant, with the entire domain being near saturation. Figure 7 shows the state of the volumetric soil moisture of the four different topographic scenarios on a day (DOY 365) after a long series of dry days, and has a wider distribution of soil moisture across the domain. Box plots of soil moisture variability on the wet and dry days were plotted for all topographies in Figure 8. On the wet day, all four domains displayed similar median soil moisture values of around 0.30 (v/v). The distribution of soil moisture values across the domains (25th to 75th quartiles) was also narrow, showing that most of the values were in the very narrow band around the median value. On the dry day, however, the median soil moisture value for each topographic scenario was different. Domains with relatively shallow sections (gentle and concave slopes) had slightly lower average soil moistures, with a greater spread of values. This clearly shows that topography has a much greater influence on the soil moisture values as the domain dries out.

[28] Each topographic scenario had different storage characteristics which were reflected in the soil moisture patterns, as well as in the flux characteristics. In the three cases with large changes in elevation across the domain, it was seen that the lowest surface locations were the driest (Figure 7). While this may appear counterintuitive with regards to the flow of water, this phenomenon is explained by the conditions imposed. Uniform evaporation and transpiration rates were applied across the entire domain. This means that the atmospheric and root water fluxes, dictated by these settings, were similar across the entire domain at any given point of time. In order to sustain this flux rate, soils at the higher elevations could draw upon the moisture stored in the vertically lower levels. However, for those soils at the lower surface elevations, the thickness of the soil profile was not available to draw upon. The bottom boundary and seepage faces also drew upon this same meager moisture resource for their fluxes. Further, no account was taken of the surface flows (run on and runoff) in this study. These fluxes can account for certain changes in soil moisture, as the state is modified on the basis of the amount of water entering or leaving a pixel, particularly at lower elevations. Hence, as no flow was contributed to the lower elevations from the higher pixels, the soils at the lower elevations dried out faster in our study.

[29] Figure 9 shows the variation of the mean soil moisture state of the domain with increase in scale. For all topographies, it was observed that the variation in the mean soil moisture value was insignificant during the wetter periods (75 and 150 days). As the domain started drying, larger discrepancies were seen in the mean soil moisture state, with the values reducing as resolution coarsened. This phenomenon was less observed in the gentle slope configuration, but was readily apparent in the other three configurations. The

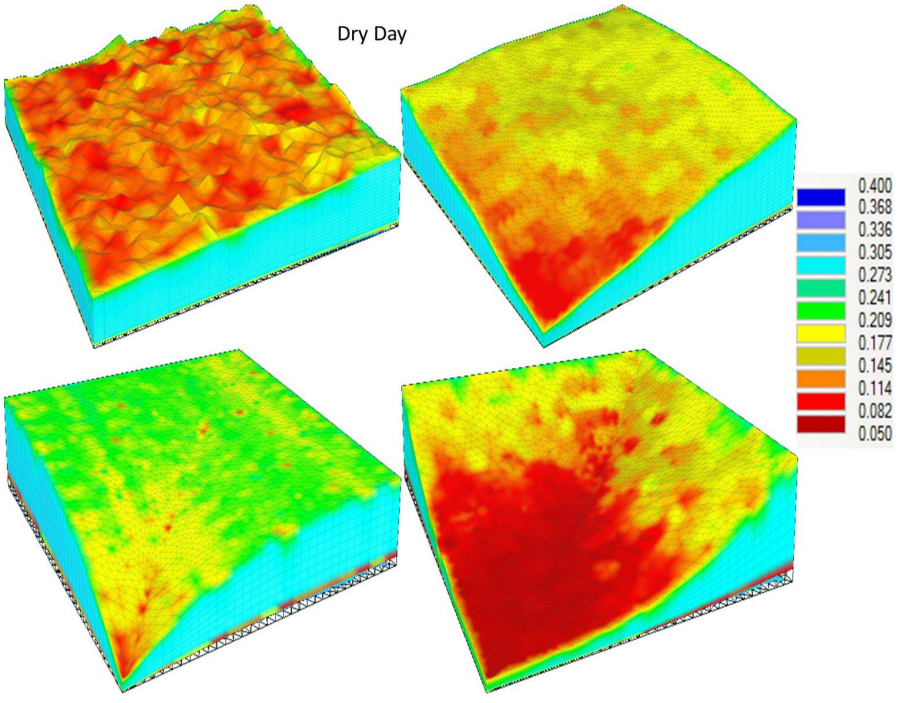

Figure 7. Soil moisture (v/v) states on a dry day for the four different topographic configurations.

gentle slope configuration was closer to a flat terrain than the others. Hence, the effect of topography on the scaled soil moisture values was seen less. However, how much of the soil moisture variation was explained by the topography alone was not evident here. *Western et al.* [1999] and *Grayson et al.* [1997] also found similar results in their studies of soil moisture and topography. They reported that the soil moisture showed a greater degree of spatial organization at the wetter end, attributed to the topography. This means that when we introduced the effect of topography into the scaling algorithm, the influence of the topography in this organization of the soil moisture pattern was accounted for. Hence, during the wetter periods, the deviation of the mean soil moisture value between scales was lessened.

[30] Statistical analyses of the soil moisture states of the study domains are given in Table 4. Although not as highly correlated with each other as the fluxes, the soil moisture states were, nevertheless, highly correlated across the scales. It was also seen that, in general, the correlation within a particular topographic configuration reduced with increasing coarseness of scale. This suggests that the upscaling algorithm employed, although generally working well, did not give us perfectly equivalent soil hydraulic parameters at coarser scales (i.e., R = 1 between soil moisture across scales). Also, the RMSE values for the soil moisture were generally low, with the highest difference being 0.049 v/v. The low RMSE values, as before, suggest that the soil moisture predictions using the upscaled effective hydraulic parameters were not significantly biased from the unscaled case. As mentioned before, the surface flows (run on and runoff) were not rerouted in this study. This could explain some of the loss of correlations between soil moisture values across scales. Since the lowest correlation obtained was 0.862 (see Table 4), we suggest that the power-averaging operator performed reasonably well for aggregating fine-scale soil hydraulic parameter values to effective, equivalent coarser-resolution values, achieving the primary objective (parameter upscaling) at hand.

3.3. Comparison of Fluxes and States From Different Initial Soil Distribution Patterns

[31] Perturbations of the initial test domains were made to generate a different distribution of the (same initial) soil materials in the domain. These cases were subjected to the same scaling and hydrologic simulation scenarios as above. This was done to test the repeatability of the test results. As expected, the soil moisture and flux patterns at the finer resolutions were slightly different from those of the first soil distribution. However, with increasing coarseness of resolution, the differences between the two soil distributions were smoothed out, and at the coarsest resolution (240 m), it was observed that the two soil moisture patterns matched very well. The mosaic of fine resolution soil properties resulted in a different pattern of surface soil moisture in the two cases. However, at coarser scales, the soil hydraulic parameters got smoothed out. Hence, where earlier a mosaic pattern was seen at the fine scale, each homogeneous coarse-scale pixel resulted in a single soil moisture value. The parameter upscaling scheme was nudging the soil hydraulic parameters toward one equivalent value. Since we are starting with a different spatial distribution of the same materials, it is logical that the coarse-scale effective parameters produce similar responses from the domain. The results obtained further validate that our topography-based scaling scheme does in fact provide effective values of soil hydraulic parameters at coarser resolutions.

3.4. Correlation With Topographic Index

[32] Computation of the compound topographic index $(\ln(A/\tan B))$ [*Beven et al.*, 1984] has been a preferred

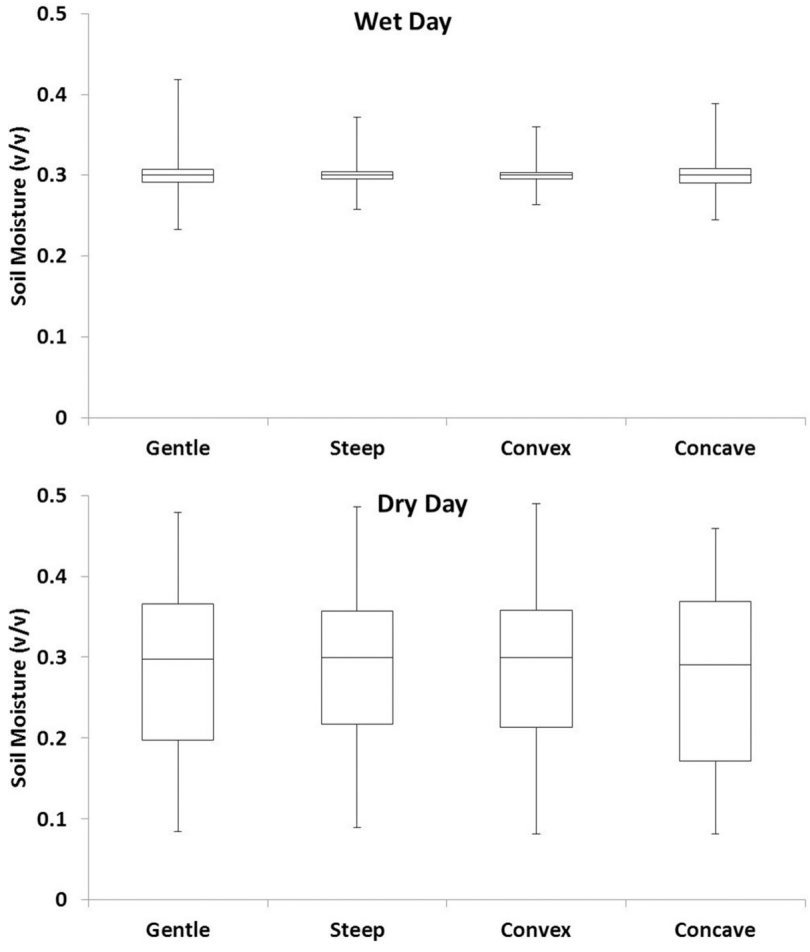

Figure 8. Box plots of soil moisture state variation on a wet and a dry day for the four different topographic configurations. The box for each topographic configuration shows the interquartile range (first to third quartile) of the soil moisture, while the whiskers represent minimum and maximum values.

mode of parameterizing the topography into a mathematical representation [*Hjerdt et al.*, 2004]. By comparing the topographic complexity of a domain, as indicated by the compound topographic index (CTI), with the variability of soil moisture and hydraulic parameters, it may be possible to derive some relationship between them. Compound topographic indices, also called wetness indices, were computed for each topographic configuration in our study. In the formulation above, A denotes the upslope catchment area per unit contour length, while tan B is the surface slope at the location. The dinf algorithm suggested by *Tarboton* [1997] was used to compute the flow direction, and thus the upslope contributing area for the CTI. This algorithm provides a more realistic representation since the flow directions are not fixed, and flow can occur in multiple directions. At each scale, the corresponding grid size (30, 60, 90, 120, and 240 m) was used to compute the CTI.

[33] Correlations of the CTI with the surface soil moisture distribution were computed at each scale at the five observation times and four topographic configurations (Figure 10). It is immediately apparent that there was no statistically significant correlation between the soil moisture pattern and the CTI. This finding is in line with those of *Western et al.* [1999], who reported that the wetness index was a poor predictor of soil moisture spatial variability. However, absence of statistical significance does not rule out physical significance. It is interesting to compare the behavior of the correlations (between CTI and surface soil moisture) with increasing scale (Figure 10). The correlations followed a general trend for each topographic configuration at all observation times. However, it was seen that the correlation plots tend to smooth out during the wetter periods (days 75 and 150), as compared to the drier periods (days 300 and 365). This phenomenon was most apparent in the gentle and concave slope topographies.

[34] Correlations between the CTI and the soil hydraulic parameters were also computed (Figure 11). It was seen that, except for the steep slope configuration, the correlations were slightly higher than those with the soil moisture. Also, the correlation plots for the van Genuchten parameters (α and n) and saturated hydraulic conductivity (K_s) were very similar. This can be explained by the fact that these three parameters may be highly interrelated. In most cases, it was also observed that the range of the correlation coefficients was narrow till the 90 m resolution, and then there was a significant variation. This observation has implications in application of the scaling methodology to

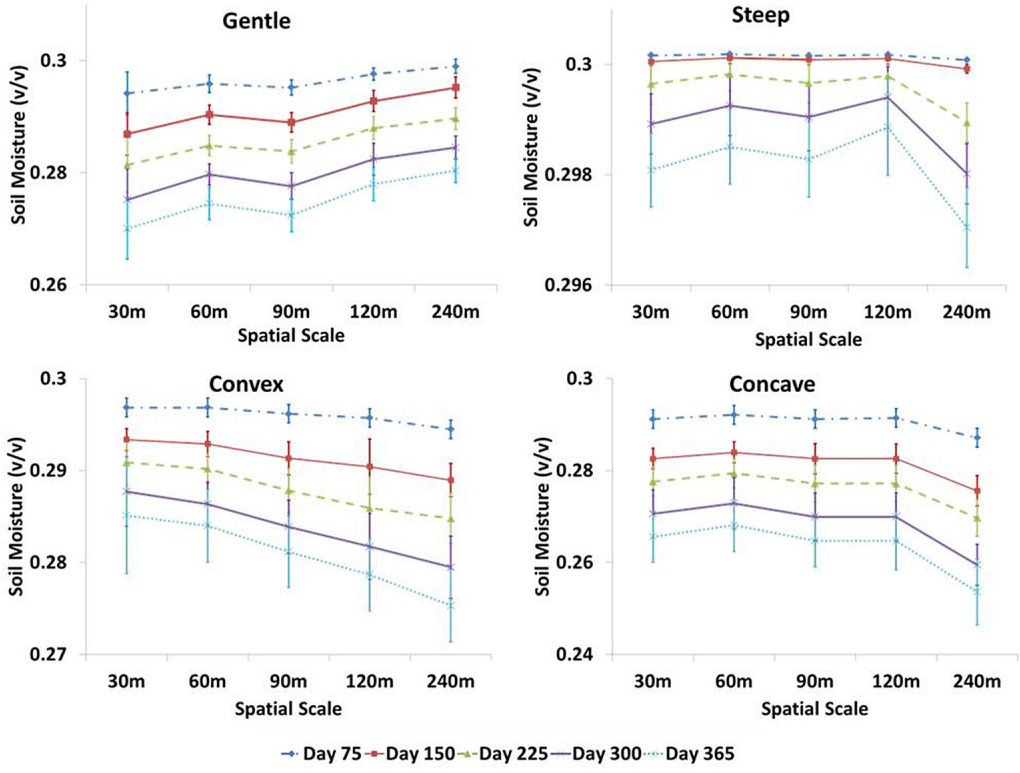

Figure 9. Mean soil moisture state variation with scale for the four different topographic configurations. Error bars represent one standard deviation.

more complex slopes. This could mean that the threshold beyond which the topography takes over dominance of the soil moisture and hydraulic parameter variability is close to this 90 m mark.

[35] Studies [*Braun et al.*, 1997; *Pradhan et al.*, 2006] have shown that the grid resolutions of the DEMs used to compute the topographic index have a significant influence on the reliability of the CTI values. As the grid sizes

Table 4. Comparative Statistics for Surface Soil Moisture States at Different Times of Simulation Using Scaled Parameters Against Unscaled (30 m) Parameters[a]

		Parameter Scale							
		60 m		90 m		120 m		240 m	
	Time	R	RMSE	R	RMSE	R	RMSE	R	RMSE
Gentle slope	75 days	0.949*	0.037	0.935*	0.011	0.927*	0.022	0.928*	0.038
	150 days	0.969*	0.031	0.961*	0.012	0.957*	0.032	0.951*	0.028
	225 days	0.965*	0.033	0.955*	0.034	0.951*	0.021	0.945*	0.025
	300 days	0.970*	0.022	0.961*	0.036	0.958*	0.019	0.952*	0.032
	365 days	0.971*	0.030	0.962*	0.047	0.959*	0.042	0.953*	0.033
Steep slope	75 days	0.958*	0.041	0.953*	0.031	0.949*	0.015	0.948*	0.013
	150 days	0.976*	0.026	0.974*	0.030	0.974*	0.031	0.972*	0.030
	225 days	0.930*	0.049	0.928*	0.032	0.928*	0.032	0.929*	0.029
	300 days	0.926*	0.035	0.926*	0.010	0.926*	0.049	0.926*	0.044
	365 days	0.907*	0.036	0.907*	0.016	0.908*	0.033	0.908*	0.019
Convex slope	75 days	0.945*	0.045	0.922*	0.030	0.874*	0.035	0.881*	0.021
	150 days	0.924*	0.013	0.892*	0.020	0.868*	0.028	0.862*	0.022
	225 days	0.933*	0.014	0.904*	0.039	0.895*	0.043	0.888*	0.043
	300 days	0.970*	0.020	0.960*	0.029	0.953*	0.030	0.948*	0.016
	365 days	0.982*	0.028	0.975*	0.047	0.968*	0.031	0.964*	0.021
Concave slope	75 days	0.932*	0.033	0.931*	0.015	0.932*	0.046	0.933*	0.011
	150 days	0.942*	0.028	0.938*	0.038	0.937*	0.035	0.936*	0.015
	225 days	0.892*	0.026	0.897*	0.011	0.896*	0.019	0.891*	0.015
	300 days	0.949*	0.038	0.947*	0.031	0.944*	0.044	0.944*	0.016
	365 days	0.937*	0.024	0.928*	0.022	0.929*	0.011	0.927*	0.041

[a]An asterisk (*) indicates correlations significant at the 0.01 level. R, Pearson's correlation coefficient; RMSE, root mean square error (v/v).

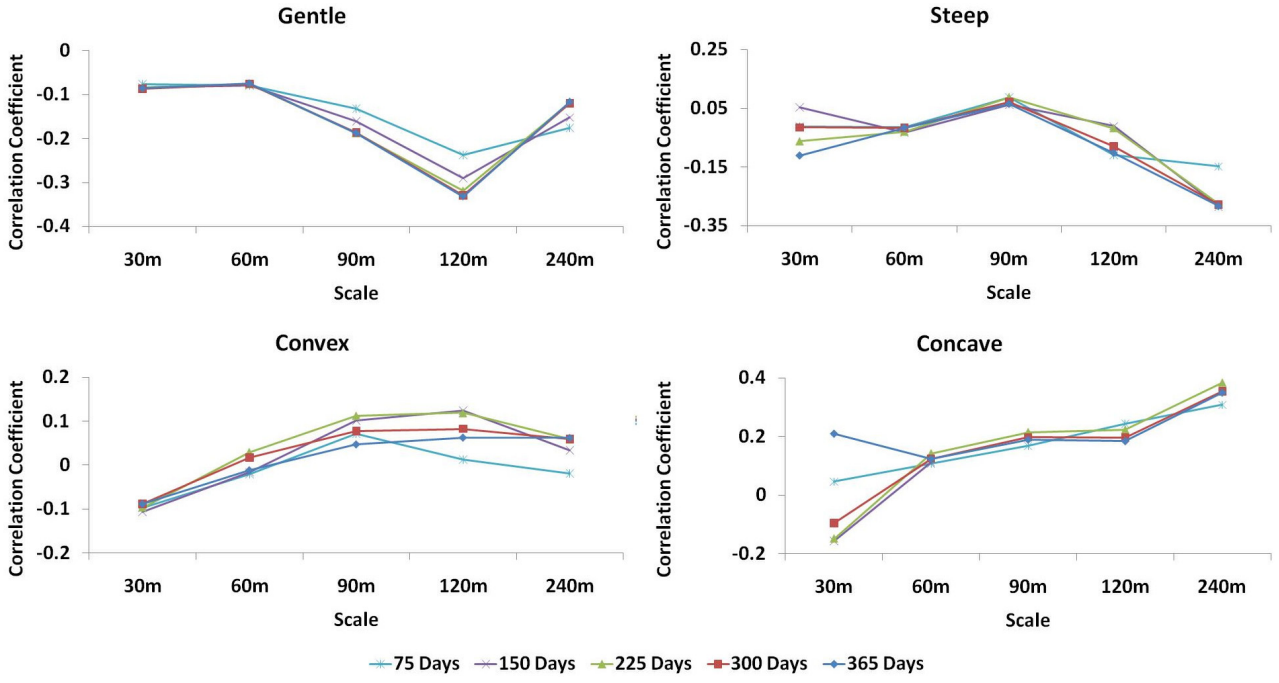

Figure 10. Correlation between compound topographic index and surface soil moisture for the four different topographic configurations.

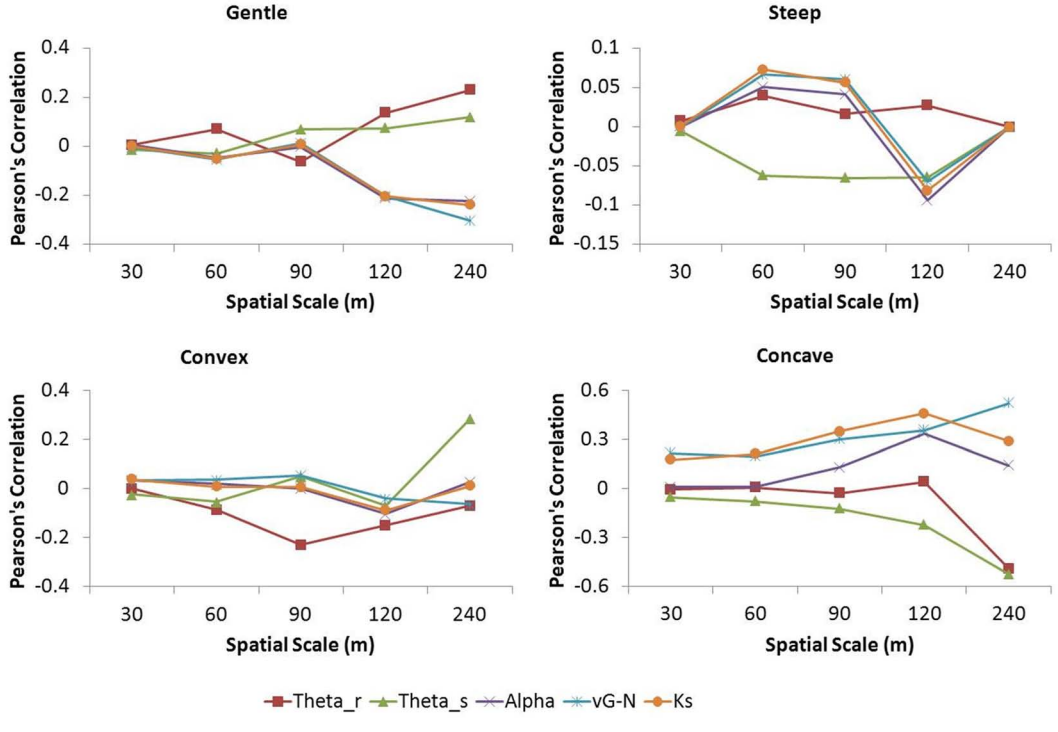

Figure 11. Correlation between compound topographic index and soil hydraulic parameters for the four different topographic configurations.

became coarser, the reliability of CTI reduced. Further, the soil moisture values also get smoothed out at the coarser resolutions. These two factors may influence the correlation values between the CTI and soil moisture.

3.5. Effect of Including Topography in the Scaling Algorithm

[36] As shown in sections 3.1 and 3.2, the topography-based scaling algorithm performed well for aggregating fine-scale soil hydraulic parameter values to effective values which honor the water fluxes and states at the coarser resolutions. We have also shown (Table 2) that the upscaled soil hydraulic parameters for the flat-terrain case were significantly different from those obtained by incorporating the topography in the scaling algorithm. However, in order to evaluate the necessity of including the topography in the upscaling algorithm, we performed another round of simulations using HYDRUS-3D. For this round, we applied the upscaled soil hydraulic parameters from the flat-terrain configuration to all four topographic scenarios. By doing so, we mimic the general practice of ignoring the topography in the scaling algorithm. While the simulation domains still had the topographic scenarios, the values of the upscaled soil hydraulic parameters assigned to the nodes were from the flat-terrain scenario. The comparative statistics for the domain fluxes and the surface soil moisture states obtained using the flat-terrain scaled inputs are provided in Tables 5 and 6. It was observed that the correlations and RMSE values for both the fluxes and the soil moisture states were similar to those reported in Tables 3 and 4 for the first two levels of upscaling (60 and 90 m). However, upon further coarsening of the support, the correlations deteriorated more perceptibly, while the RMSE values were larger, as compared to those in Tables 3 and 4. This clearly indicates that by ignoring the topography in the scaling algorithm for the coarser resolutions, we fail to account for the processes driving the soil hydraulic parameter variability at these resolutions.

[37] The concept of the threshold resolution (90 m) at which the dominant physical control shifts from soil texture and structure to topography was also further validated by these observations. In other words, soil hydraulic parameters may be effectively scaled to reflect equivalent hydrologic fluxes and soil moisture states between 30 and 90 m resolutions for the different topographic scenarios studied here without including the topography. But beyond the 90 m threshold, the inclusion of topography is necessary for improved scaling performance.

3.6. Comparison of p Norms

[38] The p norms are used to express the effective parameters in terms of the fine-scale parameters [*Zhu et al.*, 2007]. The p norm is a generalization of the common averaging schemes. The arithmetic, geometric, and harmonic averages are particular cases of the p norm. Using the method described by *Green et al.* [1996], we computed the p norms for the five soil hydraulic parameters at the different spatial scales for all four topographic scenarios as

$$P^* = \left[\left(\frac{1}{N}\right)\sum_{i=1}^{N} P_i^{p-norm}\right]^{\frac{1}{P-norm}} \quad (9)$$

where P^* is the effective parameter value at the coarse scale, P_i are the fine-scale parameter values, and N is the number of fine-scale parameter values. The computed p norm values are plotted in Figure 12 as a function of the spatial scale. The p norms for θ_r and θ_s were linear and invariant with scale. This is in line with the findings in Table 2, where it was seen that the average θ values did not change significantly with scale, or topographic scenario. The p norms for the van Genuchten α and n parameters, and the saturated hydraulic conductivity, K_s, varied nonlinearly with scale. Also, it was observed that the p norm for the van Genuchten n parameter had an increasing trend with spatial scale, while the other two parameters (α and K_s) did not show such a trend. It was also observed that the p norms for the gentle and concave slope scenarios

Table 5. Comparative Statistics for All Fluxes Using Flat-Terrain Upscaled Parameters[a]

		Parameter Scale							
		60 m		90 m		120 m		240 m	
	Slope	R	RMSE	R	RMSE	R	RMSE	R	RMSE
Atmospheric flux	gentle	0.983*	1.19E−4	0.950*	1.25E−4	0.850*	1.56E−4	0.813*	1.62E−4
	steep	0.951*	1.18E−4	0.941*	1.24E−4	0.862*	1.52E−4	0.733*	1.55E−4
	convex	0.970*	1.21E−4	0.954*	1.29E−4	0.880*	1.63E−4	0.795*	1.58E−4
	concave	0.961*	1.23E−4	0.941*	1.25E−4	0.803*	1.53E−4	0.792*	1.55E−4
Root water uptake	gentle	0.973*	1.39E−4	0.950*	1.38E−4	0.860*	1.78E−4	0.791*	1.61E−4
	steep	0.966*	1.38E−4	0.945*	1.33E−4	0.817*	1.60E−4	0.835*	1.64E−4
	convex	0.957*	1.41E−4	0.954*	1.44E−4	0.830*	1.71E−4	0.885*	1.65E−4
	concave	0.965*	1.48E−4	0.954*	1.50E−4	0.836*	1.73E−4	0.756*	1.70E−4
Drainage flux	gentle	0.951*	2.32E+2	0.944*	2.48E+2	0.718*	2.77E+2	0.797*	2.90E+2
	steep	0.927*	2.45E+2	0.943*	2.61E+2	0.853*	2.94E+2	0.865*	2.80E+2
	convex	0.960*	2.43E+2	0.944*	2.42E+2	0.763*	2.74E+2	0.742*	2.82E+2
	concave	0.964*	2.33E+2	0.965*	2.39E+2	0.847*	2.88E+2	0.847*	3.06E+2
Seepage face flux	gentle	0.956*	1.81E+1	0.931*	2.07E+1	0.751*	2.33E+1	0.743*	2.25E+1
	steep	0.933*	1.83E+1	0.928*	2.00E+1	0.857*	2.34E+1	0.786*	2.50E+1
	convex	0.908*	2.12E+1	0.871*	1.93E+1	0.809*	2.37E+1	0.813*	2.30E+1
	concave	0.930*	1.91E+1	0.927*	1.98E+1	0.846*	2.41E+1	0.786*	2.48E+1

[a]An asterisk (*) indicates correlations significant at the 0.01 level. R, Pearson's correlation coefficient; RMSE, root mean square error (m d^{-1}).

Table 6. Comparative Statistics for Surface Soil Moisture Using Flat-Terrain Scaled Parameters[a]

		Parameter Scale							
		60 m		90 m		120 m		240 m	
	Time	R	RMSE	R	RMSE	R	RMSE	R	RMSE
Gentle slope	75 days	0.906*	0.040	0.905*	0.012	0.705*	0.026	0.667*	0.045
	150 days	0.941*	0.032	0.930*	0.012	0.722*	0.038	0.689*	0.036
	225 days	0.935*	0.036	0.916*	0.036	0.708*	0.026	0.694*	0.030
	300 days	0.931*	0.022	0.922*	0.039	0.714*	0.023	0.661*	0.037
	365 days	0.941*	0.031	0.942*	0.048	0.690*	0.049	0.686*	0.041
Steep slope	75 days	0.919*	0.045	0.914*	0.033	0.720*	0.017	0.673*	0.015
	150 days	0.956*	0.028	0.925*	0.033	0.730*	0.037	0.699*	0.036
	225 days	0.892*	0.050	0.890*	0.035	0.696*	0.039	0.641*	0.035
	300 days	0.888*	0.036	0.898*	0.011	0.666*	0.058	0.638*	0.051
	365 days	0.879*	0.038	0.870*	0.016	0.690*	0.039	0.690*	0.024
Convex slope	75 days	0.916*	0.047	0.885*	0.031	0.664*	0.041	0.651*	0.026
	150 days	0.905*	0.013	0.874*	0.021	0.590*	0.036	0.594*	0.027
	225 days	0.886*	0.014	0.876*	0.042	0.662*	0.049	0.657*	0.054
	300 days	0.940*	0.022	0.940*	0.030	0.695*	0.035	0.682*	0.019
	365 days	0.952*	0.029	0.955*	0.050	0.706*	0.037	0.674*	0.025
Concave slope	75 days	0.912*	0.035	0.894*	0.015	0.699*	0.058	0.699*	0.014
	150 days	0.919*	0.029	0.894*	0.041	0.674*	0.045	0.655*	0.019
	225 days	0.861*	0.028	0.856*	0.012	0.636*	0.023	0.650*	0.019
	300 days	0.928*	0.041	0.901*	0.032	0.708*	0.054	0.670*	0.019
	365 days	0.918*	0.026	0.881*	0.024	0.706*	0.013	0.648*	0.048

[a]An asterisk (*) indicates correlations significant at the 0.01 level. R, Pearson's correlation coefficient; RMSE: root mean square error (v/v).

followed similar trends for all three hydraulic parameters. This could imply that the processes governing the soil hydraulic parameter variability in the domain behave similarly under the gentle and concave slope conditions.

3.7. Variation of Land Cover and Water Table Elevations

[39] The performance of the upscaling algorithm was tested with four different land cover types (bare soil, grass, corn, and deciduous fruit trees) in this study. It was found that while the individual land cover patterns had specific soil moisture and flux signatures, the topography-based scaling algorithm was able to provide effective soil hydraulic parameters at all scales with no modification to the form of the support function. While the flux signatures (particularly the atmospheric and root water uptake fluxes) and soil moisture patterns were different for each land cover type, similar correlations as those reported above were obtained

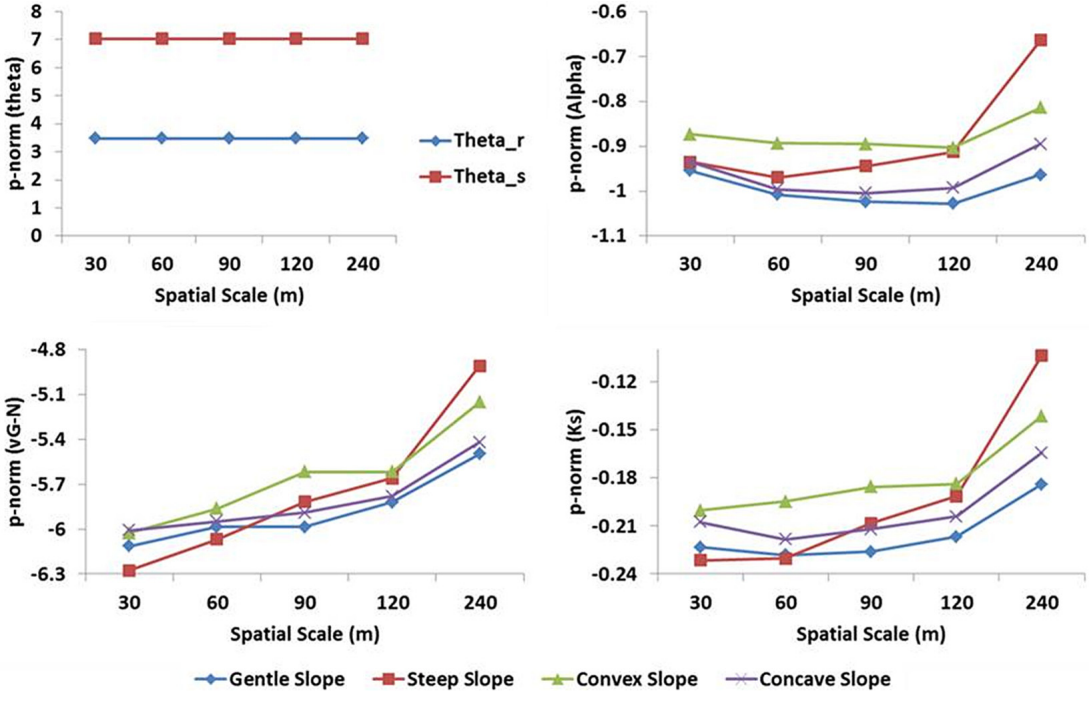

Figure 12. The p norms for scaled soil hydraulic parameters at the different spatial scales for the four different topographic configurations.

across spatial scales and times for all topographic scenarios. This suggests that the land cover pattern did not have a significant influence on the upscaling characteristics of the hydraulic parameters at the scale of the hillslope studied here. This observation is in line with our hypothesis that the soil hydraulic properties and soil moisture variability is dominated by the influence of soil texture and structure at fine scales (up to field scale), by topographic features at hillslope and/or watershed scales, and land cover (vegetation) and climate forcings (precipitation patterns) at regional scales and beyond. Similarly, the topography-based scaling algorithm performed equally well under the four different water table elevation scenarios that were tested.

[40] The above results from the suite of numerical studies suggest that the aggregation scheme, which depends mainly on the topographic characteristics of the study domain, has good potential to be used as a generic upscaling tool across topographic scenarios, soil type distributions, land cover changes, and water table elevations.

[41] Lack of perfect correlations between soil moisture and flux signatures across scales in these numerical studies may be partly explained by our choice of the scale parameter, η. The value for η was based on the linear distance between nodes in the FE mesh. However, especially at the surface, the soil formation and deposition patterns may not be linear. With nonlinear configurations such as the convex and concave slopes, the linear distance becomes an approximation of the actual travel distance and path of the water flow. However, when the two points i and j at which the parameters are aggregated are close to each other, approximation of the curved distance as a straight line may be considered reasonable. At large separations between i and j, this approximation is still justifiable because in this case, the support between p_i and p_j is small, and hence, the minor differences between the linear and curved distances may be ignored.

[42] Further, the validity of Richards' equation at such large domains under field conditions has been debated in the past [*Beven*, 2001; *Downer and Ogden*, 2003; *van Dam and Feddes*, 2000]. It has been shown that application of Richards' equation at large scales results in overestimation or underestimation of soil moisture. Since HYDRUS-3D solves for the Richards' equation for the 1000 m $\times$ 1000 m domain in our study, it is reasonable to expect some deviations from the true values for the soil moisture states at the coarser pixel scales in real-world scenarios. Further, as mentioned before, the current study did not consider the overland flow. In extending the principle to larger domains, such as watershed and beyond, this can no longer be ignored. Validation of the spatial threshold beyond which topography overtakes the dominance of soil hydraulic properties is necessary by multiple case studies in real-world scenarios.

[43] This study has considered only the effect of topography on the scaling characteristics of soil hydraulic parameters, with uniform land cover, atmospheric forcings, and water table conditions across the domain at any point of time. However, field conditions are rarely so uniform. Topographies in the real world are generally much more complex mixtures of geometries. Further, as mentioned before, the current study did not consider the overland flow. In extending the principle to larger domains, such as watershed and beyond, this can no longer be ignored. Validation of the spatial threshold beyond which topography overtakes the dominance of soil hydraulic properties is necessary by multiple case studies in real-world scenarios. In the accompanying paper [*Jana and Mohanty*, 2012], the topography-based scaling approach described here has been tested under field conditions (including lateral flow) at two different watershed-sized locations, Little Washita watershed in Oklahoma and Walnut Creek watershed in Iowa, and serves as further validation of the applicability of this scaling algorithm at large resolutions.

[44] Future work in this direction would be modification of the form of the scale parameter to incorporate more such influencing factors. Also, this algorithm may be incorporated into existing scaling schemes [e.g., *Zhu and Mohanty*, 2004] which do not consider topographic variations, to make them more comprehensive.

4. Conclusions

[45] A soil hydraulic parameter aggregation scheme based on the topographic characteristics of the study domain was formulated using the power-averaging operator algorithm. Fine-scale soil hydraulic parameters were aggregated to coarser scales in four topographic scenarios. Four plots of 1000 m $\times$ 1000 m were generated to represent hillslopes with four specific topographic configurations including gentle slope, steep slope, convex slope, and concave slope. The effectiveness of the upscaled parameters in producing similar responses for water flux and soil moisture states was tested by simulating water flow for the four domain configurations in HYDRUS-3D at different spatial resolutions.

[46] The scaled soil hydraulic parameters and the simulated soil moisture and water fluxes were compared across scale, time, soil type distribution, vegetative cover, water table elevations, and with respect to topographic indices and p norms, with good results. It was shown that topography influences the soil moisture (and, by extension, the soil hydraulic parameters) values as a domain starts drying out. It was further shown that the inclusion of topography in the hydraulic parameter scaling algorithm accounted for the variability in soil moisture and fluxes across scales for the various different conditions of soil type distribution, land cover, and water table depths. The compound topographic index (CTI) proved to be a poor estimator of the spatial variability of soil moisture. The CTI correlated slightly better with the effective soil hydraulic parameter variability, as compared with the soil moisture. More than the numerical values of the correlations, variation of the correlations with scale were of interest. Some pattern to the variation of correlation between the CTI and hydraulic parameters across scales was distinguishable. It was seen that the correlation between CTI and the effective soil hydraulic parameters changed trend beyond particular spatial scales. This observation provides validity to further investigate the use of CTI in scaling of hydraulic parameters. While the upscaling algorithm employed does not give us perfectly equivalent soil hydraulic parameters at coarser scales, reasonably good correlations are obtained. On the basis of only the topography, the scaling algorithm was able to capture much of the variation in soil hydraulic parameters

required to generate equivalent flows and soil moisture states in a coarsened domain. The similar performance of the topography-based upscaling algorithm under a variety of combinations of topographic geometry, soil type distribution, vegetation cover, and water table elevation scenarios suggests that this approach may be applicable as a general upscaling scheme for use in complex landscape conditions.

[47] **Acknowledgments.** We acknowledge the partial support of a NASA Earth System Science fellowship (NNX06AF95H), the National Science Foundation (CMG/DMS grant 062113 and C10-00021), and NASA THPs grants (NNX08AF55G and NNX09AK73G). We would also like to thank the editors and reviewers for their excellent suggestions for improving the paper.

References

Bellin, A., and Y. Rubin (1996), HYDRO_GEN: A spatially distributed random field generator for correlated properties, *Stochastic Hydrol. Hydraul.*, *10*(4), 253–278.

Beven, K. (2001), How far can we go in distributed hydrological modelling?, *Hydrol. Earth Syst. Sci.*, *5*, 1–12.

Beven, K. J., M. J. Kirkby, N. Schofield, and A. F. Tagg (1984), Testing a physically-based flood forecasting-model (TOPMODEL) for 3 UK catchments, *J. Hydrol.*, *69*(1-4), 119–143.

Bloschl, G., and M. Sivapalan (1995), Scale issues in hydrological modelling: A review, *Hydrol. Processes*, *9*, 251–290.

Braun, P., T. Molnar, and H. B. Kleeberg (1997), The problem of scaling in grid-related hydrological process modeling, *Hydrol. Process.*, *11*, 1219–1230.

Downer, C. W., and F. L. Ogden (2003), Appropriate vertical discretization of Richards' equation for two-dimensional watershed-scale modelling, *Hydrol. Earth Syst. Sci.*, *18*, 1–22.

Grayson, R. B., A. W. Western, and F. H. S. Chiew (1997), Preferred states in spatial soil moisture patterns: Local and nonlocal controls, *Water Resour. Res.*, *33*(11), 2897–2907.

Green, T. R., J. E. Constanz, and D. L. Freyberg (1996), Upscaled soil-water retention using van Genuchten's function, *J. Hydrol. Eng.*, *1*, 123–130.

Hillel, D. (1991), *Introduction to Soil Physics*, Academic Press, San Diego, Cal.

Hjerdt, K. N., J. J. McDonnell, J. Seibert, and A. Rodhe (2004), A new topographic index to quantify downslope controls on local drainage, *Water Resour. Res.*, *40*, W05602, doi:10.1029/2004WR003130.

Hopmans, J. W., D. R. Nielsen, and K. L. Bristow (2002), How useful are small-scale hydraulic property measurements for large-scale vadose zone modeling?, in *Environmental Mechanics: Water, Mass and Energy Transfer in the Biosphere, Geophys. Monogr. Ser.*, vol. 129, edited by P. A. C. Raats, D. Smiles, and A. W. Warrick, pp. 247–258, AGU, Washington, D. C.

Iorgulescu, I., and A. Musy (1997), Generalization of TOPMODEL for a power law transmissivity profile, *Hydrol. Processes*, *11*, 1353–1355.

Jana, R. B., and B. P. Mohanty (2012), A topography-based scaling algorithm for soil hydraulic parameters at hill-slope scales: Field testing, *Water Resour. Res.*, doi:10.1029/2011WR011205, in press.

Kabat, P., R. W. A. Hutjes, and R. A. Feddes (1997), The scaling characteristics of soil parameters: From plot scale heterogeneity to subgrid parameterization, *J. Hydrol.*, *190*, 363–396.

Kampf, S. K., and S. J. Burges (2007), Parameter estimation for a physics-based distributed hydrologic model using measured outflow fluxes and internal moisture states, *Water Resour. Res.*, *43*, W12414, doi:10.1029/2006WR005605.

Khaleel, R., T.-C. J. Yeh, and Z. Lu (2002), Upscaled flow and transport properties for heterogeneous unsaturated media, *Water Resour. Res.*, *38*(5), 1053, doi:10.1029/2000WR000072.

Kohnke, H., and D. P. Franzmeier (1995), *Soil Science Simplified*, 4th ed., Waveland, Long Grove, Ill.

Kuo, W.-L., T. S. Steenhuis, C. E. McCulloch, C. L. Mohler, D. A. Weinstein, S. D. DeGloria, and D. P. Swaney (1999), Effect of grid size on runoff and soil moisture for a variable-source-area hydrology model, *Water Resour. Res.*, *35*(11), 3419–3428.

Lag, J. (1951), Illustration of influence of topography on depth of A2-layer in Podzol profiles, *Soil Sci.*, *71*(2), 125–127.

Mohanty, B. P., and Z. Mousli (2000), Saturated hydraulic conductivity and soil water retention properties across a soil-slope transition, *Water Resour. Res.*, *36*(11), 3311–3324, doi:10.1029/2000WR900216.

Mohanty, B. P., and J. Zhu (2007), Effective averaging schemes for hydraulic parameters in horizontally and vertically heterogeneous soils, *J. Hydrometeorol.*, *8*(4), 715–729.

Niedda, M. (2004), Upscaling hydraulic conductivity by means of entropy of terrain curvature representation, *Water Resour. Res.*, *40*, W04206, doi:10.1029/2003WR002721.

Pradhan, N. R., Y. Tachikawa, and K. Takara (2006), A downscaling method of topographic index distribution for matching the scales of model application and parameter identification, *Hydrol. Processes*, *20*(6), 1385–1405, doi:10.1002/Hyp.6098.

Schaap, M. G., F. J. Leij, and M. T. van Genuchten (2001), Rosetta: A computer program for estimating soil hydraulic parameters with hierarchical pedotransfer functions, *J. Hydrol.*, *251*(3-4), 163–176.

Seibert, J., J. Stendahl, and R. Sørensen (2007), Topographical influences on soil properties in boreal forests, *Geoderma*, *141*(1–2), 139–148.

Shouse, P. J., and B. P. Mohanty (1998), Scaling of near-saturated hydraulic conductivity measured using disc infiltrometers, *Water Resour. Res.*, *34*(5), 1195–1205, doi:10.1029/98WR00318.

Šimůnek, J., M. T. van Genuchten, and M. Šejna (2006), The HYDRUS software package for simulating two- and three-dimensional movement of water, heat, and multiple solutes in variably-saturated media: Technical manual, version 1.0, PC-Progress, Prague.

Tarboton, D. G. (1997), A new method for the determination of flow directions and contributing areas in grid digital elevation models, *Water Resour. Res.*, *33*(2), 309–319.

Tedrow, J. C. F. (1951), Influence of topography and position on classification of soils having impeded drainage, *Soil Sci.*, *71*(6), 429–438.

van Dam, J. C., and R. A. Feddes (2000), Numerical simulation of infiltration, evaporation and shallow groundwater levels with the Richards' equation, *J. Hydrol.*, *233*, 72–85.

Vazquez, R. F., L. Feyen, J. Feyen, and J. C. Refsgaard (2002), Effect of grid size on effective parameters and model performance of the MIKE-SHE code, *Hydrol. Processes*, *16*, 355–372.

Vereecken, H., R. Kasteel, J. Vanderborght, and T. Harter (2007), Upscaling hydraulic properties and soil water flow processes in heterogeneous soils: A review, *Vadose Zone J.*, *6*, 1–28.

Western, A. W., R. B. Grayson, G. Bloschl, G. R. Willgoose, and T. A. McMahon (1999), Observed spatial organization of soil moisture and its relation to terrain indices, *Water Resour. Res.*, *35*, 797–810.

Western, A. W., S. L. Zhou, R. B. Grayson, T. A. McMahon, G. Bloschl, and D. J. Wilson (2004), Spatial correlation of soil moisture in small catchments and its relationship to dominant spatial hydrological processes, *J. Hydrol.*, *286*(1-4), 113–134, doi:10.1016/j.jhydrol.2003.09.014.

Wilson, D. J., A. W. Western, and R. B. Grayson (2004), Identifying and quantifying sources of variability in temporal and spatial soil moisture observations, *Water Resour. Res.*, *40*(2), W02507, doi:10.1029/2003WR002306.

Wu, J., and H. Li (2006), Concepts of scale and scaling, in *Scaling and Uncertainty Analysis in Ecology: Methods and Applications*, edited by J. Wu et al., pp. 3–15, Springer, Dordrecht, Netherlands.

Yager, R. R. (1996), On mean type aggregation, *IEEE Trans. Syst. Man Cybern., Part B*, *26*(2), 209–221.

Yager, R. R. (2001), The power average operator, *IEEE Trans. Syst. Man Cybern., Part A*, *31*(6), 724–731.

Yeh, T.-C. J., M. Ye, and R. Khaleel (2005), Estimation of effective unsaturated hydraulic conductivity tensor using spatial moments of observed moisture plume, *Water Resour. Res.*, *41*, W03014, doi:10.1029/2004WR003736.

Zhang, W., and D. Montgomery (1994), Digital elevation model grid size, landscape representation, and hydrologic simulations, *Water Resour. Res.*, *30*(4), 1019–1028.

Zhu, J., and B. P. Mohanty (2002a), Upscaling of soil hydraulic properties for steady state evaporation and infiltration, *Water Resour. Res.*, *38*(9), 1178, doi:10.1029/2001WR000704.

Zhu, J., and B. P. Mohanty (2002b), Spatial averaging of van Genuchten hydraulic parameters for steady-state flow in heterogeneous soils: A numerical study, *Vadose Zone J.*, *1*(2), 261–272.

Zhu, J., and B. P. Mohanty (2002c), Analytical solutions for steady state vertical infiltration, *Water Resour. Res.*, *38*(8), 1145, doi:10.1029/2001WR000398.

Zhu, J., and B. P. Mohanty (2003), Upscaling of hydraulic properties of heterogeneous soils, in *Scaling Methods in Soil Physics*, edited by Y. A. Pachepsky et al., pp. 97–118, CRC Press, Boca Raton, Fla.

Zhu, J., and B. P. Mohanty (2004), Soil hydraulic parameter upscaling for steady-state flow with root water uptake, *Vadose Zone J.*, *3*, 1464–1470.

Zhu, J., and B. P. Mohanty (2006), Effective scaling factor for transient infiltration in heterogeneous soils, *J. Hydrol.*, *319*, 96–108.

Zhu, J., B. P. Mohanty, A. W. Warrick, and M. T. van Genuchten (2004), Correspondence and upscaling of hydraulic functions for steady-state flow in heterogeneous soils, *Vadose Zone J.*, *3*, 527–533.

Zhu, J., B. P. Mohanty, and N. N. Das (2006), On the effective averaging schemes of hydraulic properties at the landscape scale, *Vadose Zone J.*, *5*, 308–316.

Zhu, J., M. H. Young, and M. T. van Genuchten (2007), Upscaling schemes and relationships for the Gardner and van Genuchten hydraulic functions for heterogeneous soils, *Vadose Zone J.*, *6*, 186–195.

R. B. Jana and B. P. Mohanty, Department of Biological and Agricultural Engineering, Texas A&M University, 142 Scoates Hall, MS 2117, College Station, TX 77843-2117, USA. (bmohanty@tamu.edu)